Received: 9 September 2019 | Revised: 17 December 2019 | Accepted: 7 January 2020

DOI: 10.1111/jnc.14960

ORIGINAL ARTICLE

Journal of Neurochemistry JNC The Official Journal of the International Society for Neurochemistry WILEY

Sleep deprivation regulates availability of PrP^C and Aβ peptides which can impair interaction between PrP^C and laminin and neuronal plasticity

Marcio H. M. da Luz[1] | Jessica M. V. Pino[1] | Tiago G. Santos[2] | Hanna K. M. Antunes[3] | Vilma R. Martins[2] | Altay A. L. de Souza[3] | Ricardo J. S. Torquato[1] | Kil S. Lee[1]

[1]Department of Biochemistry, Universidade Federal de São Paulo, São Paulo, Brazil

[2]International Research Center. A.C.Camargo Cancer Center, São Paulo, Brazil

[3]Department of Psychobiology, Universidade Federal de São Paulo, São Paulo, Brazil

Correspondence
Kil S. Lee, Department of Biochemistry, Universidade Federal de São Paulo, Rua Pedro de Toledo 669, 8° andar, Vila Clementino, São Paulo, SP, Brazil.
Email: kslee@unifesp.br

Funding information
This study was supported by grants from FAPESP (Fundação de Amparo à Pesquisa do Estado de São Paulo: 2016/04297-6 and 2017/10404-2), CNPq (467566/2014-3), and Coordenação de Aperfeiçoamento de Pessoal de Nível Superior—Brasil (CAPES)—Finance Code 001.

Abstract

PrP^C is a glycoprotein capable to interact with several molecules and mediates diverse signaling pathways. Among numerous ligands, laminin (LN) is known to promote neurite outgrowth and memory consolidation, while amyloid-beta oligomers (Aβo) trigger synaptic dysfunction. In both pathways, mGluR1 is recruited as co-receptor. The involvement of PrP^C/mGluR1 in these opposite functions suggests that this complex is a key element in the regulation of synaptic activity. Considering that sleep-wake cycle is important for synaptic homeostasis, we aimed to investigate how sleep deprivation affects the expression of PrP^C and its ligands, laminin, Aβo, and mGluR1, a multicomplex that can interfere with neuronal plasticity. To address this question, hippocampi of control (CT) and sleep deprived (SD) C57BL/6 mice were collected at two time points of circadian period (13 hr and 21 hr). We observed that sleep deprivation reduced PrP^C and mGluR1 levels with higher effect in active state (21 hr). Sleep deprivation also caused accumulation of Aβ peptides in rest period (13 hr), while laminin levels were not affected. In vitro binding assay showed that Aβo can compete with LN for PrP^C binding. The influence of Aβo was also observed in neuritogenesis. LN alone promoted longer neurite outgrowth than non-treated cells in both $Prnp^{+/+}$ and $Prnp^{0/0}$ genotypes. Aβo alone did not show any effects, but when added together with LN, it attenuated the effects of LN only in $Prnp^{+/+}$ cells. Altogether, our findings indicate that sleep deprivation regulates the availability of PrP^C and Aβ peptides, and based on our in vitro assays, these alterations induced by sleep deprivation can negatively affect LN–PrP^C interaction, which is known to play roles in neuronal plasticity.

KEYWORDS

Aβ peptides, laminin, prion protein, synaptic plasticity

Abbreviations: 95CI, 95% confidence interval; AD, Alzheimer's disease; APP, amyloid precursor protein; Aβo, amyloid-beta oligomers; BACE1, β-secretase 1; BPTI, bovine pancreatic trypsin inhibitor; CTact, control group of activity period; CTrest, control group of rest period; ERK, extracellular signal-regulated kinases; FBS, fetal bovine serum; LN, laminin; mGLuR1, metabotropic glutamate receptor 1; NMDAR, N-methyl-D-aspartate receptor; PrP^C, cellular prion protein; rPrP, recombinant prion protein; RRID, research resource identifier; SD, sleep deprivation/deprived; SDact, sleep deprived group of activity period; SDrest, sleep deprived group of rest period.

1 | INTRODUCTION

One of the common features observed in neurodegenerative diseases is aggregation and deposition of specific proteins such as infectious prion protein in transmissible spongiform encephalopathies (Yi, Xu, Chen, & Liang, 2013), Tau in Alzheimer´s disease (Iqbal et al., 2005) and α-synuclein in Parkinson´s disease (Spillantini & Goedert, 2000). Normal functions of these proteins are often related to cell survival, differentiation, and neuronal activities (Bendor, Logan, & Edwards, 2013) (Guo, Noble, & Hanger, 2017) (Wulf, Senatore, & Aguzzi, 2017).

In the case of prion protein (PrP^C), several studies have described its functions in signaling pathways related to synaptic plasticity, neurotransmission, cell proliferation and differentiation (Linden et al., 2008). These pleiotropic functions of PrP^C are dependent of various ligands and co-receptors. For instance, laminin 1, which is composed of α1, β1, and γ1 chains and most abundant form in brain, binds to PrP^C with high affinity. This interaction promotes neuronal plasticity and memory consolidation via extracellular signal-regulated kinases (ERK) pathway (Colognato & Yurchenco, 2000) (Graner et al., 2000). Particularly, hippocampus is one of the brain areas where laminin is abundantly expressed and the disruption of PrP^C–laminin interaction in hippocampus impairs memory retention (Coitinho et al., 2006). On the other hand, the interaction between PrP^C and oligomers of Aβ peptide (Aβo) can inhibit hippocampal long-term potentiation leading to synaptic dysfunction by activating Fyn kinase and N-methyl-D-aspartate receptor (NMDAR) (Lauren, Gimbel, Nygaard, Gilbert, & Strittmatter, 2009) (Um et al., 2012). In both cases, metabotropic glutamate receptor 1 (mGluR1) is recruited as a co-receptor (Beraldo, Arantes, & Santos, 2011) (Um, Kaufman, & Kostylev, 2013). These findings suggest that PrP^C/mGluR1 complex is an important element for the regulation of synaptic activities, and depending on the availability of specific ligands, these two proteins can be engaged in opposite processes.

Another common feature associated with neurodegenerative diseases is disruption of circadian rhythm (Musiek, 2015) (Leng, Musiek, Hu, Cappuccio, & Yaffe, 2019). Several factors can impair sleep-wake cycle in neurodegenerative diseases. For example, the expression of mutant PrP^C can cause abnormal sleep pattern (Dossena et al., 2008), while the expression of wild-type PrP^C is regulated along circadian period (Cagampang et al., 1999). In patients with Alzheimer's disease (AD), higher levels of orexin have been observed (Liguori et al., 2014). This neurotransmitter that promotes wakefulness can also increase the production of Aβ peptide (Liguori, 2017) (Kang et al., 2009). Thus, prolonged wakefulness caused by sleep deprivation can increase the levels of Aβ peptide. Corroborating these findings, sleep deprivation has been pointed as one of the risk factors for neurodegenerative diseases (Wu, Dunnett, Ho, & Chang, 2019), while adequate sleep is known to be important for hippocampal-dependent memory consolidation (Marshall & Born, 2007) (Diekelmann & Born, 2010) (Havekes & Abel, 2017) (Sawangjit et al., 2018).

Based on this evidence, we aimed to evaluate the levels of PrP^C, laminin, and Aβ peptides in sleep deprived animals, and to investigate the influence of Aβo on the interaction between LN and PrP^C using in vitro assays to better understand how PrP^C, Aβ, and laminin can contribute to the regulation of neuronal plasticity in hippocampus upon sleep deprivation.

2 | METHODS

2.1 | Materials

2.1.1 | Reagents

Acetic acid (Synth, Cat# A1019.01.BJ); Acrylamide (Sigma-Aldrich, Cat# 01700); B-27™ Supplement (ThermoFisher Scientific, Cat# 17504044); β-Amyloid peptide (1–42, human sequence) (Calbiochem, Cat# PP69); Bovine serum albumin (BSA) (Inlab, Cat# 1870); Bromophenol Blue (Nuclear, Cat# 311663); Dimethyl sulfoxide (DMSO) (Synth, Cat# 01D1011.01.BJ); EDTA (Calbiochem, Cat# 34103); Fetal bovine serum (ThermoFisher Scientific, Cat# 16140071); Fluorsave reagent (Calbiochem, Cat# 345789); Glycerol (Synth, Cat# G1005.01.BJ); Glycine (Sigma-Aldrich, Cat# G7126); Ham's F12 Nutrient (Cultilab, Cat# H0269); Hexafluoroisopropanol (HFIP) (Sigma-Aldrich, Cat# 52512); Image-iT fixative solution (ThermoFisher Scientific, Cat# R37814); Laminin (Sigma-Aldrich, Cat# L2020); L-Glutamine (ThermoFisher Scientific, Cat# 25030149); Luminata Forte Western HRP substrate (Merck-Millipore, Cat# WBLUF0100); Neurobasal medium (ThermoFisher Scientific, Cat# 21103049); Methanol (Merck-Millipore, Cat# 106007); NaCl (Labsynth, Cat# C1060.01.AM); N,N′-Methylenebis-acrylamide (Sigma-Aldrich, Cat# 146072); PBS (Sigma-Aldrich, Cat# P4417); Penicillin-Streptomycin (ThermoFisher Scientific, Cat# 15140122); Phosphatase Inhibitor Cocktail (Calbiochem, Cat# 78428); Poly-L-lysine (Sigma-Aldrich, Cat# P4832); Protease Inhibitor Cocktail (Calbiochem, Cat# 539131); Sodium deoxycholate (Sigma-Aldrich, Cat# D6750); TMB substrate (Amresco, Cat# K830); Triton x-100 (Sigma-Aldrich, Cat# T8787); Trizma base (Sigma-Aldrich, Cat# 93352); Trypsin (ThermoFisher Scientific, Cat# 25200056); Tween-20 (Sigma-Aldrich, Cat# P1379).

2.1.2 | Primary antibodies

Anti-alpha-tubulin (Cell Signaling Technology Cat# 2125, RRID: AB_2619646); anti-APP (Cell Signaling Technology Cat# 2452, RRID: AB_10694227); anti-BACE (Cell Signaling Technology Cat# 5606, RRID: AB_1903900); anti-β-amyloid 1–42 (diluted 1:2000; Cell Signaling, Cat# D3E10); anti-Erk1/2 (Cell Signaling Technology Cat# 9102, RRID: AB_330744); anti-GAPDH (Cell Signaling Technology Cat# 2118, RRID: AB_561053); anti-laminin (Abcam Cat# ab11575, RRID: AB_298179); anti-mGluR1 (Cell Signaling Technology Cat# 12551, RRID: AB_2797953); anti-NMDAR2B (Cell Signaling Technology Cat# 4212, RRID: AB_2112463); anti-phospho-Erk1/2 (Cell Signaling Technology Cat# 9101, RRID:

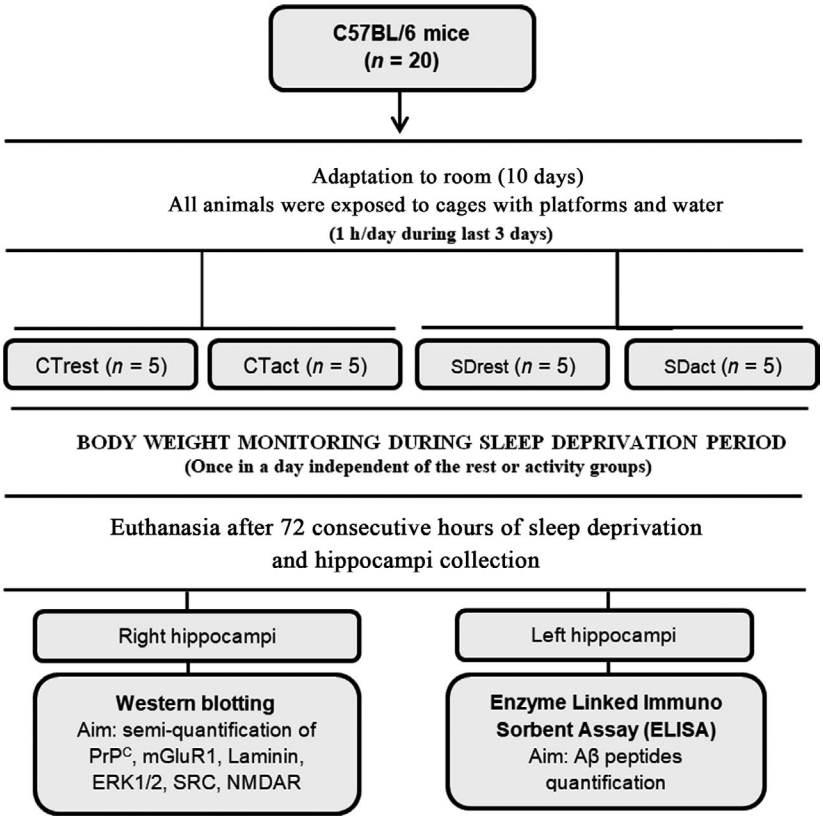

FIGURE 1 Experimental flowchart for sleep deprivation. The flowchart shows timeline of procedures, number of animals used in each group, and measurements carried out with the samples. Whole experiment was replicated to complete 10 animals per group. However, one right hippocampus of each group was used for other experiment not reported in this study, and one additional right hippocampus of CTrest group was lost during the sample preparation

AB_331646); anti-phospho-NMDAR2B (Cell Signaling Technology Cat# 4208, RRID: AB_1549657); anti-phospho-Src (Cell Signaling Technology Cat# 6943, RRID: AB_10013641); anti-prion protein (Cayman Chemical Cat# 189720–1, RRID: AB_327961); anti-Src (Cell Signaling Technology Cat# 2123, RRID:AB_2106047).

2.1.3 | Secondary antibodies

Anti-Mouse IgG-Peroxidase antibody (Sigma-Aldrich Cat# A4416, RRID:AB_258167); anti-Rabbit IgG-Peroxidase antibody (Sigma-Aldrich Cat# A6154, RRID:AB_258284).

2.1.4 | Others

96-well plate (GreinerBio-One, Cat# 655081); ELISA kits (Invitrogen, Cat#KMB3481; Cat#KMB3441); Nunc™ Lab-Tek™ II Chamber Slide™ System (ThermoFisher Scientific, Cat# 154526); PVDF membrane (Sigma-Aldrich, Cat# IPVH00010).

2.2 | Animals

For sleep deprivation protocol, male C57BL/6 mice (RRID: IMSR_JAX:000664) with 3 months of age were obtained from Center for Development of Experimental Models for Medicine and Biology (CEDEME/UNIFESP). *Prnp* knockout mice used in neurite outgrowth assay were obtained from A.C.Camargo Cancer Center. These animals were descendants from the ZrchI line (RRID: MGI:2174709) (Bueler et al., 1992). Wild-type mice were generated by crossing descendants of an initial mating between 129/SvEvBrd and C57BL/6J. Genotyping was routinely carried out as described in our previous study (Lima et al., 2007). Briefly, Knockout mice were identified amplifying neomycin gene using primers 5′-TTGAGCCTGGCGAACAGTTC-3′ and 5′-GATGGATTGCACGCAGGTTC-3′ under the following cycling condition: 94°C–5 min; 35 cycles of 94°C–1 min, 57°C–1 min, and 72°C–45 s; final extension of 72°C–5 min. Wild-type mice were confirmed by the amplification of PrP gene using primers 5′-AACCGTTACCCACCTCAGGGT-3′ and 5′-GCGCTCCATCATCTTCACA-3′ under the following cycling condition: 94°C–1 min; 35 cycles of 94°C–1 min, 60°C–1 min, and 72°C–45 s; final extension of 72°C–5 min. To avoid false negative results, all amplifications were performed in multiplex using primers 5′-AATAGAGGCACTCCCTTCAC-3′ and 5′-GGTAAGCCCTTGACCTAAAA-3′ that target retinoblastoma gene. All experimental procedures were approved by the Research Ethics Committee of UNIFESP (N 9806251113) and by the Research Ethics Committee of A.C.Camargo Cancer Center (N 077/17).

2.3 | Sleep deprivation

Male C57BL/6 mice were housed in temperature controlled room (22 ± 2°C) with 12:12 hr light/dark cycle. Light phase started at 07:00 a.m. Animals were adapted in the room for 10 days. During the last

3 days of adaptation, all animals (including control group) were exposed to the cage constructed for sleep deprivation for 1 hr/day. Sleep deprivation protocol was carried out for 72 consecutive hours using multiple platforms method adapted for mice (Guariniello, Vicari, Lee, Oliveira, & Tufik, 2012). Five animals were placed in a cage (38 × 31 × 17 cm) containing nine circular platforms (1.5 cm of diameter) and shallow water. This setting allows animals to move freely between the platforms. However, when animals enter in paradoxical sleep, they fall into the water as a result of muscle atonia and are awaken. Food and water were offered ad libitum during the entire experimental period. After sleep deprivation, animals were killed by decapitation without the use of anesthesia, and hippocampi were rapidly dissected, frozen on dry ice, and stored in −80°C until use. The experiment consisted of four groups: control animals killed at 13 hr (CTrest) and at 21 hr (CTact); Sleep-deprived animals killed at 13 hr (SDrest) and at 21 hr (SDact). Thirteen hours corresponds to zeitgeber time 6 (ZT6) and resting period of rodents. Twenty-one hours corresponds to ZT14 and active period. For this study, total of 40 animals were used (10 animals per group). To minimize anecdotal differences between the groups that may occur as a result of the experimental procedures, samples were collected using two batches of animals (Figure 1). Each cage containing five animals was arbitrarily assigned to one of four experimental groups. Euthanasia and tissue collection lasted less than 20 min for each time, and the order of the groups to be killed was inverted between the experiments. No exclusion criteria were predetermined, and none of the animals died or were excluded during the experimental period. One hippocampus of each group was used to test the isolation of raft membrane, which will not be reported in this study. One additional hippocampus of CTrest group was lost during the sample preparation and the sample was not replaced. To minimize distress, all animals provided in a same cage were allocated to one of the experimental groups without matching by body weight. Also, the animals were adapted to the room and sleep deprivation apparatus prior to carrying out the experiments and they were always handled by the same person during the experimental procedure. This study was not pre-registered.

2.4 | Western blot

Hippocampi were homogenized in lysis buffer (Tris 100 mM pH 8.0, NaCl 150 mM, Triton x-100 1%, EDTA 10 mM, Sodium deoxycholate 0.5%, Protease Inhibitor Cocktail, and Phosphatase Inhibitor Cocktail). Lysate was centrifuged for 5 min at 2700 g and 4°C, and supernatant was collected. Proteins of the lysates were fractionated by SDS-PAGE using 10 or 12% polyacrylamide gel and transferred to PVDF membrane. Membrane was incubated with 5% of bovine serum albumin (BSA) in TBS-T (Tris 50 mM, NaCl 150 mM, Tween-20 0.1%, pH 7.4) for 1 hr at 20 – 24°C, and then, with primary antibody for 1 hr at 20 – 24°C or overnight at 4°C. After three washes with TBS-T for 5 min each, membrane was incubated with peroxidase-conjugated secondary antibody for 1 hr, and then washed five times with TBS-T. The signals were developed using Luminata Forte Western HRP substrate. Images of membrane were acquired using UVITEC Imaging System (Cambridge; Alliance mini 4 m). Band intensity of the proteins of interest was normalized using Ponceau S staining, which was quantified using Image J v.1.50i. All primary antibodies were used in working dilution of 1:1,000, except for anti-alpha tubulin (1:5,000), anti-GAPDH (1:10,000), anti-phospho-ERK1/2 (1:500), anti-phospho-NMDAR (1:500), and anti-phospho-SRC (1:500). Secondary antibodies were diluted 1:10,000.

2.5 | Immunoenzymatic assay (ELISA)

Aβ40 e Aβ42 peptides were analyzed using commercial ELISA kits (Invitrogen, Cat#KMB3481; Cat#KMB3441). Hippocampus was homogenized in 70 µl of Tris-HCl 50mM (pH 8.0) containing 5 M Guanidine-HCl, and incubated for 4 hr at room temperature (20°C to 24°C). Samples were then diluted in Dulbecco's Phosphate-Buffered Saline (DPBS) containing 5% of BSA and 0.03% of Tween-20 (1:50). After dilution, samples were centrifuged for 20 min at 16,000 g and 4°C. Supernatants (100 µl) were added to antibody-adsorbed wells and incubated for 2 hr. After washes, detection antibody was added and incubated for 1 hr. Signals were developed using a secondary antibody conjugated with peroxidase and TMB substrate provided in the kits. After adding stop solution, absorbance was measured at 450 nm. For data analysis, the amount of each peptide (Aβ40 e Aβ42) was summed up and then, normalized with respective CTrest. Two independent experiments were performed using two batches of animals (Figure 1).

2.6 | Aβ peptides oligomerization

β-Amyloid peptide 1–42 (0.25 mg) was dissolved in 55.4 µl of HFIP and kept at room temperature (20°C to 24°C) until complete evaporation of HFIP, which took approximately 3 hr. This procedure is known to favor the maintenance of monomeric form of the peptides (Chromy, Nowak, & Lambert, 2003). Then, peptide was reconstituted with DMSO at 1 mM (4.5 µg/µl) as described by Caetano et al., (2011). To generate oligomers, DMSO reconstituted peptides were diluted in Ham's F12 Nutrient (Cultilab H0296) to 100 µM (0.45 µg/µl), incubated for 24 hr in 4°C. Ham's F12 Nutrient contained 3 µM of phenol red which is far below the IC50 that can inhibit oligomerization (~400 µM) (Necula, Kayed, Milton, & Glabe, 2007). The preparation was stored at −80°C in aliquots of 20 µl. All experiments were performed using freshly thawed aliquots as done in previous study (Caetano et al., 2011). The storage of Aβo prep at −80°C did not change the oligomeric states compared with fresh Aβo prep (Figure S1). Prior to use, the aliquots were centrifuged at 5,000 g for 20 s.

2.7 | Non-denaturing page

Non-denaturing PAGE was performed as described by Arndt and colleagues (Arndt, Koristka, Bartsch, & Bachmann, 2012). 0.9 µg of aged Aβ peptides were diluted in 2x sample buffer (Tris-HCl 0.187 M, pH 6.8, glycerol 30%, and Bromophenol Blue), and then loaded into

8%–20% gradient gel. Electrophoresis was carried out using Tris-Glycine buffer (25 mM Tris; 192 mM Glycine).

2.8 | Size exclusion chromatography

Aged Aβ peptides (27 nmol in 270 µl of Ham's F12 Nutrient containing 10% of DMSO) were fractionated using a Superdex 75 10/300 GL column (Äkta Purifier, GE Healthcare life Science). PBS was used as liquid phase at a flow rate of 0.4 ml/min. Elution of Aβ oligomers was monitored by absorbance at 215 nm. The column was calibrated with bovine serum albumin (67 kDa), ovalbumin (45 kDa), Carbonic anhydrase (29 kDa), Cytochrome C (12.4 kDa), and bovine pancreatic trypsin inhibitor (6.5 kDa). Void volume was established with blue dextran (2000 kDa).

2.9 | Silver staining

Polyacrylamide gels were fixed for 20 min with methanol 50% containing 5% of acetic acid, and then washed with methanol 50% followed by Milli-Q water. A sodium thiosulfate 0.02% was used for 1 min to sensitize gels and then rinsed with Milli-Q water twice. Gels were incubated with silver nitrate 0.1% for 20 min and washed twice with Milli-Q water. Staining was developed with sodium carbonate 3% containing 0.04% of formaldehyde. When appropriate color was developed, reaction was stopped with acetic acid 5%. Gels were washed with acetic acid 1% and then with Milli-Q water.

2.10 | Binding assay

Binding assays were performed as described in previous study with some modifications (Graner et al., 2000). Recombinant PrP (rPrP) or BSA was adsorbed onto 96-well plate. Based on the protein binding capacity of the plate, we assumed that 200 ng (or 8.7 pmol) of rPrP was adsorbed into each well. After blocking unspecific binding sites with BSA 1% diluted in PBS for an hour, the blocking solution was removed. Then, 50 µl of blocking solution containing 0.4, 0.8, 1.2, or 1.6 pmol of laminin was added in each well. For blank control, 50 µl of blocking solution was added without laminin. Freshly thawed Aβo was also added into selected wells (7 and 14 pmol in 50 µl of blocking solution). In wells where Aβo was not added, 50 µl of blocking solution was added to complete final volume of 100 µl and incubated for 2 hr. The amount of 7 and 14 pmol of Aβo was empirically chosen to cover equimolar range of rPrP. After three washes with PBS, BSA 1% was added and incubated for 1 hr. And then, anti-laminin (diluted 1:2000) or anti-β-amyloid 1–42 (diluted 1:2000) was added and incubated for 1 hr. After four washes with PBS, peroxidase-conjugated secondary antibody diluted 1:5,000 was added and incubated for 1 hr. After four washes with PBS, TMB substrate was added and incubated in the dark for 5–10 min. Reaction was stopped using acidic solution. Absorbance was measured at 450 nm. To calculate mole for Aβo solutions, molecular weight of pentamer (22.4 kDa) was used, as the most abundant species in aged solution migrated as ~20 kDa (Figure 7a). For LN solution, 810 kDa was used as its molecular weight, and for rPrP, 23 kDa was used.

2.11 | Neurite outgrowth assay

Experimental design is presented in Figure 2. Hippocampi derived from fetus (E17) were incubated in trypsin 0.25% for 10 min with constant shaking and then pellet was washed with neurobasal medium containing 10% of fetal bovine serum. After gentle hydromechanical dissociation, cells were stained with trypan blue and counted. For neurite outgrowth assay, 2×10^4 cells were seeded in each well of Nunc™ Lab-Tek™ II Chamber Slide™ System previously treated with poly-L-lysine 5 µg/µl. The cells were maintained

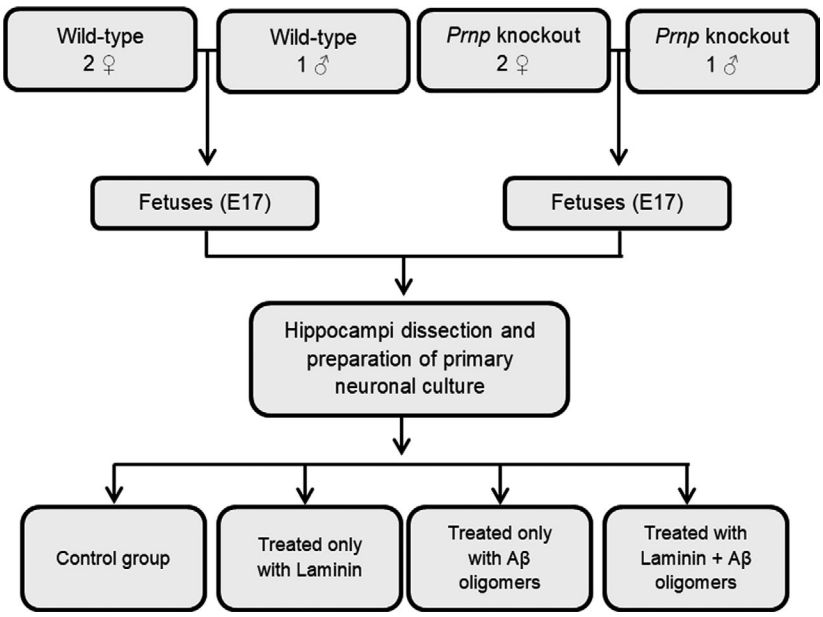

FIGURE 2 Experimental flowchart for neurite outgrowth assays. The flowchart shows the source of hippocampal cells of two genotypes and the treatments applied to the cells

in neurobasal media supplemented with Penicillin-Streptomycin 1%, L-Glutamine 1%, and B-27™ Supplement 2%, where laminin 0.01 μM and/or Aβo 0.14 μM were added and incubated for 24 hr at 37°C with 5% CO_2 in humidified chamber. After the treatment, cells were fixed with Image-iT fixative solution and stained with hematoxylin. Slides were mounted with cover glass using Fluorsave reagent. Images were acquired on Nikon Eclipse TE2000-U microscope using 20× objective lens.

2.12 | Data analysis

Body weight was analyzed with repeated measures ANOVA test followed by Duncan post hoc. For the graphical analysis of the body weight and western blot data, individual data and the mean differences among groups with bootstrap 95% confidence interval (95CI) were calculated using DABEST package implemented in a web application framework (Ho, Tumkaya, Aryal, Choi, & Claridge-Chang, 2019). LN-PrP^C binding assay, which was performed with multiple concentrations of laminin, was presented as mean ± 95CI. For neurite outgrowth assay, images of three independent experiments were analyzed using NeuronJ plugin of Image J v.1.50i. Neurites of each cell were manually traced and measured. Approximately 150–300 cells were analyzed per group in each experiment. For each independent experiment, average length of neurite was calculated, and 2 (genotypes) × 3 (treatment) ANOVA was applied followed by a Duncan post hoc. For all hypothesis testing analysis, Statistica v.13 software (STATISTICA, RRID: SCR_014213) was used and the level of significance was set as 5% for all analysis ($p < .05$). Interquartile range (IQR) was used to determine outliers. According to these criteria, an outlier was removed only from Aβ peptides data. The authors were not blinded to perform the experiments and to analyze the data. Sample size was empirically determined. To assess the normality of dependent variable, we opted to use Q-Q plots and visual method to verify the lack of data skewness instead of normality test based on p-values as Shapiro-Wilk or K-S tests (Loy, Follett, & Hofmann, 2016).

2.13 | Data and material sharing

All custom-made materials and raw data will be shared upon reasonable request.

3 | RESULTS

3.1 | Effects of sleep on expression of PrP^C, mGluR1 and related signaling molecules

To investigate effects of sleep on the expression of molecules that participate in PrP^C/mGluR1 signaling, animals were subjected to sleep deprivation. As described in previous studies (Koban & Swinson, 2005) (Monico-Neto et al., 2015), abrupt reduction in body weight was observed in the first 24 hr of sleep deprivation with continuous loss in subsequent days (Figure 3a, orange). After 3 days of protocol, control animals gained 0.43 ± 0.08 g ($n = 20$), whereas sleep deprived animals lost 2.13 ± 0.21 g ($n = 20$) (Figure 3b). The mean difference between the groups was −2.56 and its 95CI was depicted with black vertical line on the right axis (Figure 3b).

To quantify the protein levels in distinct sleep/wake states, hippocampi of control and sleep deprived animals were collected at two circadian time points: 13:00 hr as resting condition and 21:00 hr as active condition. Thus, we had four groups for molecular analysis: Control group collected at 13 hr (CTrest) and 21 hr (CTact) and sleep deprived group collected at 13 hr (SDrest) and 21 hr (SDact). The study design is represented in Figure 1. Planned comparisons were performed between active and resting conditions within the same experimental groups (CT and SD) or between CT and SD within the same circadian time, calculating mean differences (effect size) with respective 95CI (Ho et al., 2019).

Figure 4a shows a representative image of western blot for PrP^C and Figure 4b shows relative PrP^C levels of individual samples in the groups. PrP^C levels did not vary between two circadian time points in both CT and SD groups (Figure 4c; CTrest minus CTact or SDrest minus SDact). However, sleep deprivation reduced PrP^C levels compared with respective CT groups in both circadian times (Figure 4c; SDrest minus CTrest or SDact minus CTact). Regarding mGluR1 levels, higher mean difference was observed between SDact and CTact (Figure 4d–f). The values of mean differences and respective 95CI were described in the figure legends.

Laminin 1 which is a ligand of PrP^C did not undergo drastic changes by distinct circadian times, neither by sleep deprivation (Figure 4g–i). On the other hand, Aβ peptides levels, measured by ELISA, were increased in SDrest group compared with CTrest (Figure 4j–k). Aβ peptide is derived from proteolytic cleavage of amyloid precursor protein (APP) and β-secretase 1 (BACE1) is one of the key enzymes. APP levels were reduced in CTact compared with CTrest (Figure 4l–n). This effect of circadian time was attenuated by sleep deprivation, and both SD groups showed lower levels of APP compared with respective CT groups (Figure 4l–n). Similarly, BACE1 levels were also different between two circadian time points in CT groups, and this time-dependent variation was attenuated in SD groups (Figure 4o–q). However, unlike APP, BACE1 levels were increased in SDact group compared with CTact (Figure 4o–q). This alteration of BACE1 in sleep deprived animals could influence the APP processing and production of Aβ peptides.

Subsequently, we investigated phosphorylation degree of related signaling molecules previously described, which include ERK1/2, SRC family kinase that include Fyn kinase, and subunit NR2B of NMDAR (Beraldo et al., 2011) (Um et al., 2012). More evident difference was observed in ERK1/2 levels between SDrest and CTrest group (Figure 5a–c). Similar difference was also observed in SRC kinases, that is, higher phosphorylation degree in SDrest compared with CTrest (Figure 5d–e). However, owing to the high coefficient

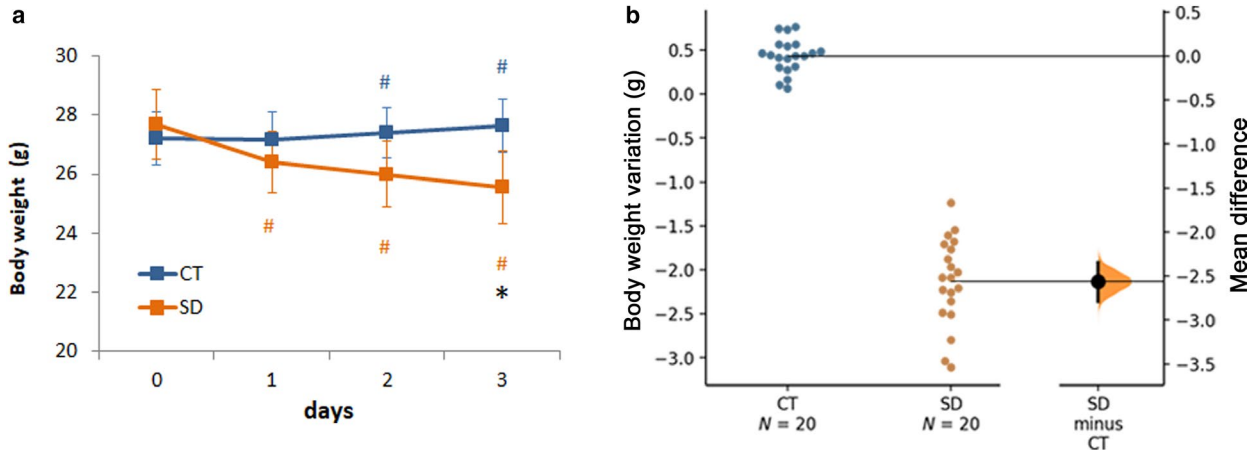

FIGURE 3 Body weight variation during sleep deprivation period. (a) Mean body weight of control (CT, n = 20) and sleep deprived (SD, n = 20) animals were represented with respective 95CI. Data were analyzed by Repeated Measures ANOVA followed by Duncan's post hoc analysis. Asterisk (*) indicates $p \leq .05$ in the comparison between CT and SD on designated day. Symbol # indicates $p \leq .05$ in the comparison with previous measurement. (b) Body weight variation was calculated subtracting body weight of last day from the body weight of first day (n = 20 per group). Body weight variation of both groups is plotted on the left axes and the mean difference between groups is plotted on the right axes as a bootstrap sampling distribution. The mean difference is depicted as a black dot and the 95CI is indicated by the vertical error bar. The unpaired mean difference between CT and SD was −2.56 [95CI: −2.79, −2.35]

of variation of the groups, this difference was not as evident as the ERK1/2 (Figure 5f, SDrest minus CTrest). Regarding the NMDAR phosphorylation, subtle reduction was observed in SDact compared with CTact (Figure 5g–i).

For the molecular analysis shown in Figure 4, total protein content detected by Ponceau S staining was used as normalization factor, as two commonly used loading controls, GAPDH (Figure 6a–c) and α-Tubulin (Figure 6d–f), were affected by both circadian time and sleep deprivation as evidenced by the mean differences observed between the groups (Figure 6c and f).

In summary, these results showed that prolonged wakefulness reduced PrP^C and mGluR1 with higher effect in active condition, and increased Aβ peptide levels and ERK1/2 phosphorylation with higher effect in resting condition.

3.2 | Aβo compete with LN for PrP^C binding and impact on neuritogenesis

Increased Aβ peptide levels promote their aggregation, generating oligomers that can bind with PrP^C (Lauren et al., 2009), (Dohler et al., 2014). Thus, reduced PrP^C levels and increased Aβ peptide levels would displace the interaction between LN and PrP^C if both LN and Aβo could compete with each other for PrP^C binding. To test this hypothesis, synthetic Aβ 1–42 peptide was submitted to spontaneous oligomerization in HAM's F12 medium as previously described (Chromy et al., 2003) with some modifications described in methods section. Analysis of the sample by non-denaturing gel electrophoresis showed an oligomer of ~20 kDa as the most abundant species (Figure 7a). The sample was also analyzed by size exclusion chromatography. Major portion of the oligomers was eluted in void volume (peak A) and in volume that correspond to 13 kDa (peak B, Figure S1). This fractionation profile was very similar to what was observed by Chromy et.al., including the size difference observed between two approaches (Chromy et al., 2003).

Recombinant PrP (rPrP) was adsorbed onto 96-well plate, and laminin solutions with distinct concentration were added to each well. Bound laminin was detected using antibody anti-laminin. A dose-dependent binding was observed with increased laminin concentrations (Figure 7b, blue). In presence of 7 pmol of Aβo, less laminin was bound to rPrP (Figure 7b, orange), and 14 pmol of Aβo promoted an even higher inhibition (Figure 7b, green). Similar assay was also performed using anti-Aβ which detects bound Aβo. As shown in Figure 7c, the presence of laminin also reduced the binding of Aβo. Upper panel shows measurement of each replicate, and lower panel shows the mean difference between the designated groups. These results demonstrate that laminin and Aβo compete with each other for PrP^C binding.

To investigate some biological meaning of this competition, neurite outgrowth in vitro assay was performed using primary neurons derived from wild-type or *Prnp* knockout mice (Figure 7d–e). The study design is represented in Figure 2. The number of neurite per neuron or percentage of neurons with neurite was not different either between the groups or the genotypes. However, laminin promoted longer neurite outgrowth in both cell types compared with respective non-treated cells, and Aβo peptides alone did not show any effects (Figure 7d). When laminin and Aβo were added simultaneously, both cell types still showed longer neurite than their respective non-treated group. However, when compared with respective laminin-treated group, only wild-type cells showed shorter neurites (Figure 7d). These data indicate that presence of Aβo attenuated laminin effect in PrP^C-dependent manner, and support the results of binding assay.

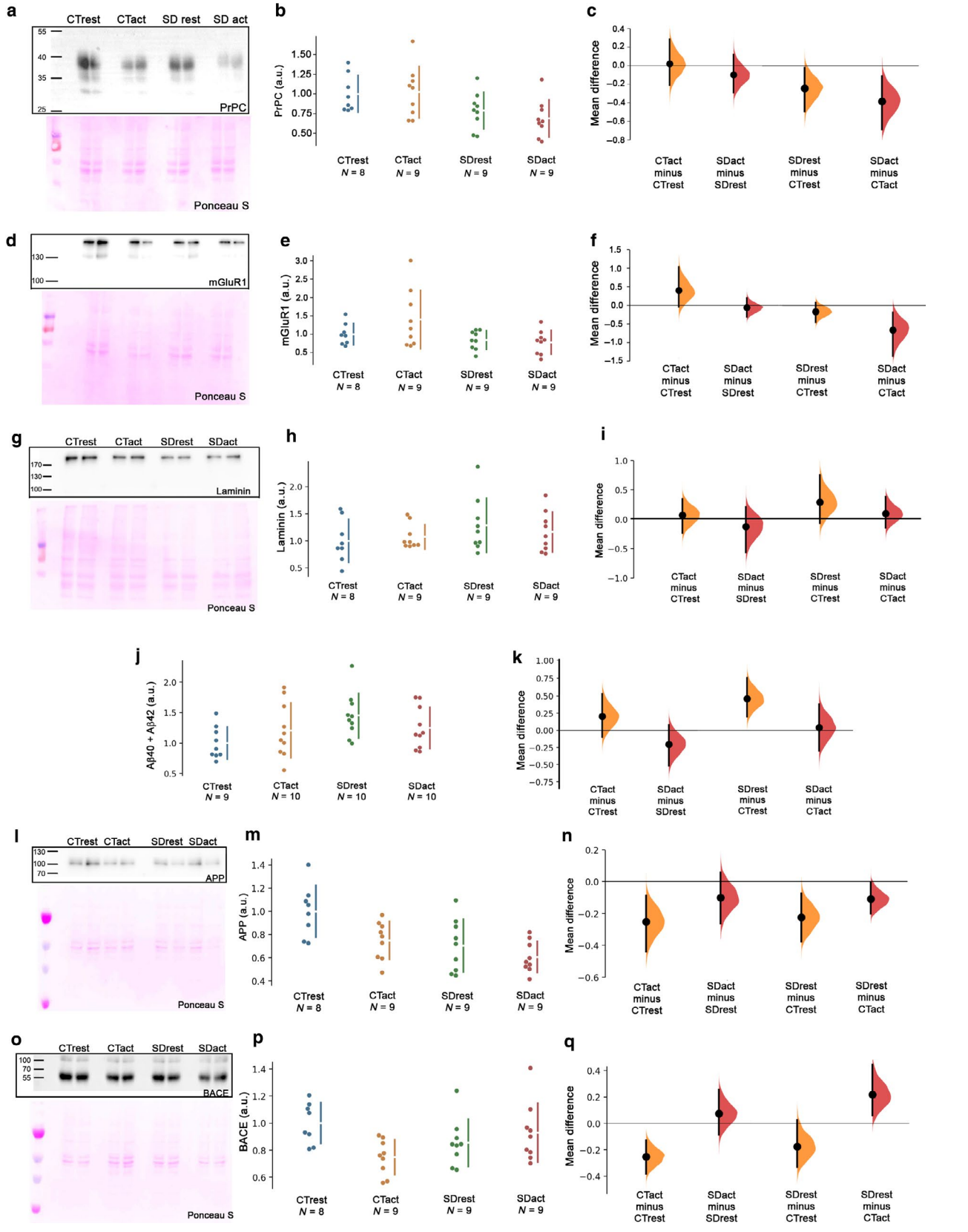

4 | DISCUSSION

The main goal of this study was to understand how laminin and Aβo can trigger opposite phenomena using the same receptor PrP^C/mGluR1. Based on previous studies that reported effects of sleep deprivation on metabolism of Aβ peptides and importance of PrP^C in the regulation of circadian rhythm, we aimed to investigate the relative availability of laminin, Aβ peptides, PrP^C, and mGluR1 in control and sleep deprived animals.

FIGURE 4 Levels of PrP^C, Aβ peptide, and related proteins upon sleep deprivation. (a, d, g, l, and o) Representative images of western blots of PrPC, metabotropic glutamate receptor 1, Laminin, amyloid precursor protein (APP), and BACE with respective Ponceau S staining. (b, e, h, j, m, and p) Relative levels of PrPC, metabotropic glutamate receptor 1, Laminin, APP, BACE, and Aβ peptides. Relative levels of Aβ peptides were assessed by ELISA. Each dot represents an individual mouse (N = 8 for CTrest group and N = 9 for other groups). (c, f, i, k, n, and q) The mean difference between the designated groups was plotted as a bootstrap sampling distribution and it is depicted as a black dot. Vertical error bar represents 95CI. (c) The unpaired mean difference between CTrest and CTact was 0.0222 [95CI: −0.209, 0.283]; between SDrest and SDact was −0.0987 [95CI: −0.292, 0.12]; between CTrest and SDrest was −0.213 [95CI: −0.43, −0.0195]; and between CTact and SDact was −0.334 [95CI: −0.599, −0.0981]. (f) The unpaired mean difference between CTrest and CTact was 0.4 [95CI: −0.0407, 1.03]; between SDrest and SDact was −0.0636 [95CI: −0.309, 0.197]; between CTrest and SDrest was −0.158 [95CI: −0.428, 0.0637]; and between CTact and SDact was −0.622 [95CI: −1.27, −0.181]. (i) The unpaired mean difference between CTrest and CTact was 0.07 [95CI: −0.234, 0.35]; between SDrest and SDact was −0.124 [95CI: −0.562, 0.206]; between CTrest and SDrest was 0.285 [95CI: −0.0759, 0.744]; and between CTact and SDact was 0.0906 [95CI: −0.157, 0.376]. (k) The unpaired mean difference between CTrest and CTact was 0.205 [95CI: −0.0996, 0.532]; between SDrest and SDact was −0.202 [95CI: −0.515, 0.0783] between CTrest and SDrest was 0.449 [95CI: 0.196, 0.741]; and between CTact and SDact was 0.0422 [95CI: −0.288, 0.372]. (n) The unpaired mean difference between CTrest and CTact was −0.252 [95CI: −0.439, −0.0888]; between SDrest and SDact was −0.1 [95CI: −0.265, 0.0575]; between CTrest and SDrest was −0.213 [95CI: −0.43, −0.0195]; and between CTact and SDact was −0.224 [95CI: −0.375, −0.0753]. (q) The unpaired mean difference between CTrest and CTact was −0.253 [95CI: −0.382, −0.127]; between SDrest and SDact was 0.0733 [95CI: −0.0867, 0.254]; between CTrest and SDrest was −0.145 [95CI: −0.276, 0.0219], and between CTact and SDact was 0.181 [95CI: 0.0514, 0.368]

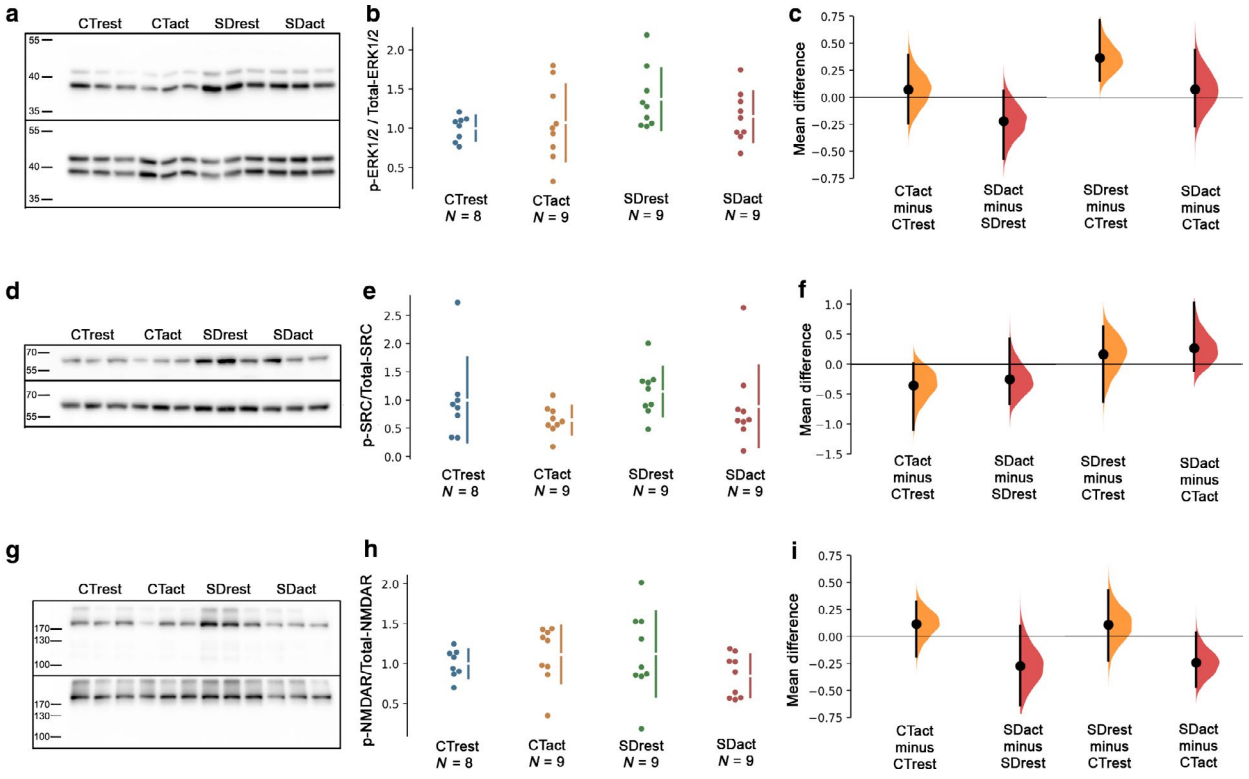

FIGURE 5 Phosphorylation levels of extracellular signal-regulated kinases (ERK)1/2, SRC, and N-methyl-D-aspartate receptor (NMDAR). (a, d, and g) Representative images of western blots for phosphorylated (upper panels) and total (lower panels) ERK1/2, SRC, and NMDAR. (b, e, and h) Relative ratio of phosphorylated proteins to total proteins. Each dot represents an individual mouse (n = 8 for CTrest group and n = 9 for other groups). (c). The mean difference between the designated groups in phosphorylation degree of ERK1/2 was plotted as a bootstrap sampling distribution and it is depicted as a black dot. Vertical error bar represents 95CI. The unpaired mean difference between CTrest and CTact was 0.0689 [95CI: −0.245, 0.392]; between SDrest and SDact was −0.221 [95CI: −0.568, 0.061]; between CTrest and SDrest was 0.368 [95CI: 0.157, 0.717]; and between CTact and SDact was 0.0785 [95CI: −0.266, 0.438]. (f) The mean difference between the designated groups in phosphorylation degree of SRC was plotted as a bootstrap sampling distribution and it is depicted as a black dot. Vertical error bar represents 95CI. The unpaired mean difference between CTrest and CTact was −0.355 [95CI: −1.1, 0.0101]; between SDrest and SDact was −0.257 [95CI: −0.668, 0.422]; between CTrest and SDrest was 0.146 [95CI: −0.576, 0.569]; and between CTact and SDact was 0.244 [95CI: −0.104, 0.932]. (i) The mean difference between the designated groups in phosphorylation degree of NMDAR was plotted as a bootstrap sampling distribution and it is depicted as a black dot. Vertical error bar represents 95CI. The unpaired mean difference between CTrest and CTact was 0.114 [95CI: −0.185, 0.322]; between SDrest and SDact was −0.274 [95CI: −0.637, 0.0967]; between CTrest and SDrest was 0.124 [95CI: −0.252, 0.484]; and between CTact and SDact was −0.275 [95CI: −0.526, 0.0401]

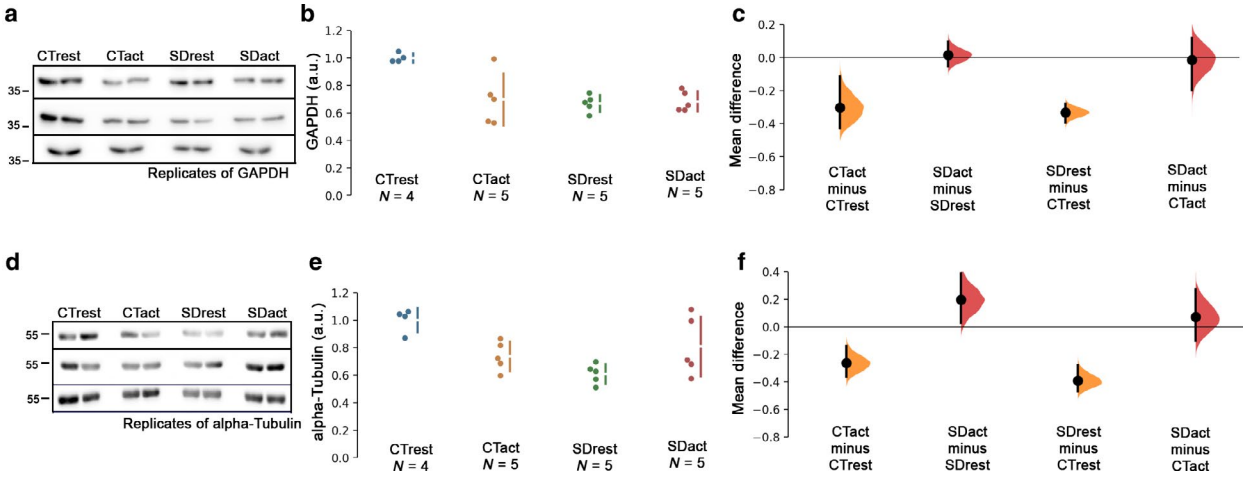

FIGURE 6 Effect of SD on GAPDH and α-tubulin levels. (a and d) Three representative images of western blots for GAPDH and α-tubulin. (b and e) Relative GAPDH and α-tubulin levels. Each dot represents an individual mouse (n = 4 for CTrest group and n = 5 for other groups). (c). The mean difference between the designated groups in GAPDH levels was plotted as a bootstrap sampling distribution and it is depicted as a black dot. Vertical error bar represents 95CI. The unpaired mean difference between CTrest and CTact was −0.303 [95CI: −0.426, −0.114]; between SDrest and SDact was 0.0156 [95CI: −0.0546, 0.0973]; between CTrest and SDrest was −0.332 [95CI: −0.392, −0.282]; and between CTact and SDact was −0.0136 [95CI: −0.199, 0.12]. (f) The mean difference between the designated groups in α-tubulin levels was plotted as a bootstrap sampling distribution and it is depicted as a black dot. Vertical error bar represents 95CI. The unpaired mean difference between CTrest and CTact was −0.263 [95CI: −0.366, −0.14]; between SDrest and SDact was 0.198 [95CI: 0.031, 0.387]; between CTrest and SDrest was −0.391 [95CI: −0.469, −0.277]; and between CTact and SDact was 0.0702 [95CI: −0.103, 0.273]

PrP^C expression varies along circadian period at mRNA levels with higher expression at zeitgeber time 14 (Cagampang et al., 1999). This time point corresponds to 21:00 hr of our study. However, in our study, protein levels of PrP^C did not vary between two time points (13:00 hr vs. 21:00 hr). Since Cagampang and colleagues used rats in their study, we cannot rule out that this divergent observation occurred as a result of the species difference. However, divergences between quantity of mRNA and protein levels have been already reported in other studies (Denman, Potempska, Wolfe, Ramakrishna, & Miller, 1991) (Ford et al., 2002). Thus, it is possible that PrP^C expression is regulated at both mRNA and protein levels.

In addition, we observed that sleep deprivation significantly reduced PrP^C levels. This reduction can impair PrP^C interaction with its ligands. On the other hand, the levels of Aβ peptides were increased by sleep deprivation. This augment can compensate the reduction in PrP^C. Thus, these results suggest that sleep deprived condition can favor the interaction between Aβo-PrP^C than between LN-PrP^C.

Our in vitro binding assay indicated that increased amount of Aβo can hinder the interaction between laminin and PrP^C, despite distinct binding sites of both ligands (Coitinho et al., 2006) (Lauren et al., 2009). Beraldo and colleagues have reported that both ligands do not compete. However, this study was carried out using a peptide derived from γ1 chain of laminin (Beraldo et al., 2011) (Lauren et al., 2009). In our study, we used whole laminin 1 which is a macromolecule of ~800 kDa composed of α1, β1, and γ1 chains, and more abundant form in brain (Colognato & Yurchenco, 2000). Of note, when Aβo are prepared using synthetic peptide, species of ~20 kDa appears to show higher affinity to PrP^C (Dohler et al., 2014). Thus, considering that PrP^C is relatively small protein, it is reasonable to predict that competition between LN and Aβo occurred as a result of steric hindrance.

Lastly, we observed that LN promoted neurite outgrowth of both genotypes in a similar manner, and Aβo alone did not impair neurite outgrowth of both cell types. Neurotoxicity of Aβo is related with size and structure of oligomers and can widely vary between preparations (Cizas et al., 2010) (Sandberg, Luheshi, & Sollvander, 2010) (Choi et al., 2013) (Diociaiuti et al., 2014). Oligomers used in this study probably did not hold neurotoxic activity, but they were able to attenuate LN-induced neuritogenesis only in wild-type cells. These results reinforce previous studies that have demonstrated that laminin promotes neurite outgrowth partially via PrP^C (Beraldo et al., 2011), which can be hindered in the presence of Aβo. Therefore, conditions that increase the concentration of Aβo can impair the neurite outgrowth promoted by PrP^C-LN interaction. Of note, these neurite outgrowth assays were performed using *Prnp* knockout mice and control mice with mixed genetic background of 129S7/SvEvBrd and C57BL/6. Although one can claim that heterogeneous genetic background might influence the results, our previous findings show that PrP^C-dependent neuritogenesis are very similarly reproduced using C57BL/10 control and knockout mice (Lima et al., 2007) (Arantes et al., 2009).

In this study, we showed that sleep deprivation reduced PrP^C expression and increased the level of Aβ peptides. We also showed that Aβo impaired the interaction between PrP^C and LN, and LN-induced neuritogenesis in wild-type cells. It is well described that prolonged sleep debt impairs cognitive functions. As interaction of laminin with PrP^C is important for synaptic plasticity and memory consolidation (Coitinho et al., 2006), reduction in PrP^C level, accumulation of Aβ peptides, and consequent disruption of PrP^C-laminin

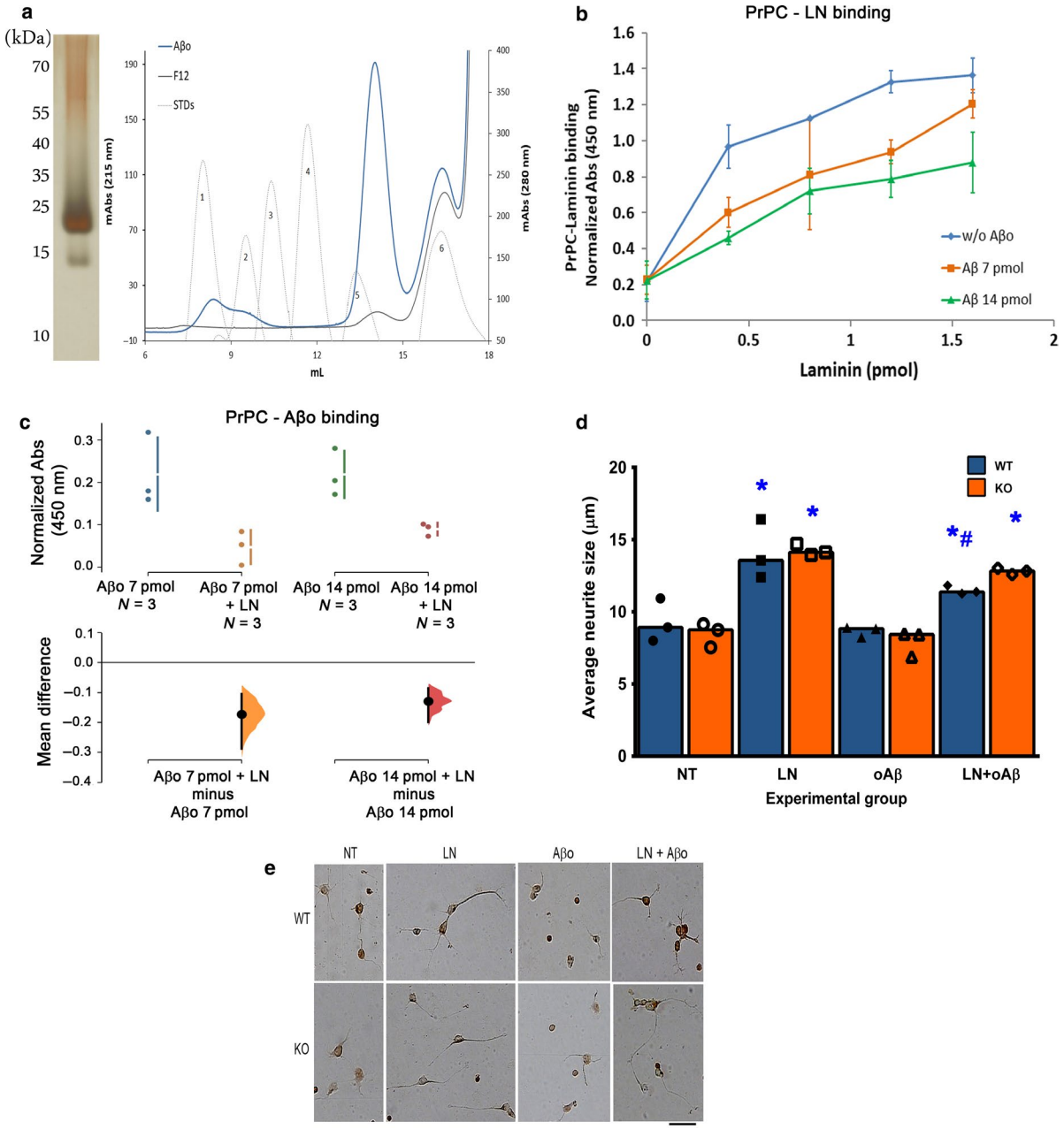

FIGURE 7 In vitro binding assays and neurite outgrowth assays. (a) Oligomers of Aβ1-42 peptide was prepared as described in methods section and stored at −80°C. To analyze oligomeric state of this preparation, the material was freshly thawed and subjected to non-denaturing PAGE using 8%–20% gradient gel, which was further stained with silver nitrate. The material was also analyzed by size-exclusion chromatography (blue line). HAM's F12 medium used to dilute Aβ peptide was also analyzed (gray line). Dashed lines show calibration standards (1- Blue Dextran (2.000 kDa); 2- BSA (67 kDa); 3- Ovalbumin (45 kDa); 4- Carbonic Anhydrase (29 kDa); 5- Cytochrome C (12.4 kDa); and 6- bovine pancreatic trypsin inhibitor (6.5 kDa)). As a result of the lack of tryptophan residues in Aβ peptide, elution of this peptide was monitored by absorbance at 215 nm (left axis). Calibration standards were monitored at 280 nm (right axis). (b) Laminin was added to recombinant prion protein (rPrP) adsorbed onto 96-well plate in absence (blue) or presence of Aβo 7 pmol (orange) and 14 pmol (green). Bound laminin (LN) was detected using anti-Laminin. Each data point represents mean ± 95CI. (c) Similar assay was performed using anti-Aβ antibody to detect bound oligomers. Scatter plot shows results of three independent experiments (upper panel). The mean difference between the designated groups in binding capacity was plotted as a bootstrap sampling distribution and it is depicted as a black dot. Vertical error bar represents 95CI. The unpaired mean difference between Aβo 7 pmol and Aβo 7 pmol + LN was −0.173 [95CI: −0.288, −0.104] and between Aβo 14 pmol and Aβo 14 pmol + LN was −0.129 [95CI: −0.199, −0.0857. (d) Primary neurons derived from wild-type (WT) or Prnp knockout (KO) mice were divided into four groups: cells treated for 24 hr with LN or Aβo alone, or with both ligands (LN + Aβo), and non-treated cells (NT). Mean neurite length of the groups of each independent experiment is shown by dot. Bar graph represents the mean of three independent experiments. Data were analyzed by two-way ANOVA. No significant difference was observed between the genotypes. Asterisk (*) indicates $p \leq .05$ in comparison with respective NT. Symbol # indicates $p \leq .05$ in comparison with respective LN group. (e) Representative images of neurite outgrowth assay. Bar = 10 μm

binding might be a part of molecular mechanisms that lead to low cognitive performance in sleep deprived individuals.

ACKNOWLEDGMENTS AND CONFLICT OF INTEREST DISCLOSURE

We thank Dr. Aparecida Sadae Tanaka (Department of Biochemistry, UNIFESP) that have kindly permitted us to use equipment and reagents for size exclusion chromatography. Vilma Regina Martins is an editor for Journal of Neurochemistry. Otherwise, the authors do not have competing interests related to this study.

All experiments were conducted in compliance with the ARRIVE guidelines.

OPEN RESEARCH BADGES

This article has received a badge for *Open Materials* because it provided all relevant information to reproduce the study in the manuscript. More information about the Open Science badges can be found at https://cos.io/our-services/open-science-badges/.

ORCID

Marcio H. M. da Luz https://orcid.org/0000-0001-8203-2572
Tiago G. Santos https://orcid.org/0000-0001-6641-7413
Vilma R. Martins https://orcid.org/0000-0002-2909-8502
Kil S. Lee https://orcid.org/0000-0002-2390-2774

REFERENCES

Arantes, C., Nomizo, R., Lopes, M. H., Hajj, G. N., Lima, F. R., & Martins, V. R. (2009). Prion protein and its ligand stress inducible protein 1 regulate astrocyte development. *Glia*, *57*, 1439–1449. https://doi.org/10.1002/glia.20861

Arndt, C., Koristka, S., Bartsch, H., & Bachmann, M. (2012). Native polyacrylamide gels. *Methods in Molecular Biology*, *869*, 49–53.

Bendor, J. T., Logan, T. P., & Edwards, R. H. (2013). The function of alpha-synuclein. *Neuron*, *79*, 1044–1066.

Beraldo, F. H., Arantes, C. P., Santos, T. G., Machado, C. F., Roffe, M., Hajj, G. N., … Martins, V. R. (2011). Metabotropic glutamate receptors transduce signals for neurite outgrowth after binding of the prion protein to laminin gamma1 chain. *The FASEB Journal*, *25*, 265–279.

Bueler, H., Fischer, M., Lang, Y., Bluethmann, H., Lipp, H. P., DeArmond, S. J., … Weissmann, C. (1992). Normal development and behaviour of mice lacking the neuronal cell-surface PrP protein. *Nature*, *356*, 577–582. https://doi.org/10.1038/356577a0

Caetano, F. A., Beraldo, F. H., Hajj, G. N. M., Guimaraes, A. L., Jürgensen, S., Wasilewska-Sampaio, A. P., … Prado, M. A. M. (2011). Amyloid-beta oligomers increase the localization of prion protein at the cell surface. *Journal of Neurochemistry*, *117*, 538–553. https://doi.org/10.1111/j.1471-4159.2011.07225.x

Cagampang, F. R., Whatley, S. A., Mitchell, A. L., Powell, J. F., Campbell, I. C., & Coen, C. W. (1999). Circadian regulation of prion protein messenger RNA in the rat forebrain: A widespread and synchronous rhythm. *Neuroscience*, *91*, 1201–1204. https://doi.org/10.1016/S0306-4522(99)00092-5

Choi, Y. J., Chae, S., Kim, J. H., Barald, K. F., Park, J. Y., & Lee, S. H. (2013). Neurotoxic amyloid beta oligomeric assemblies recreated in microfluidic platform with interstitial level of slow flow. *Scientific Reports*, *3*, 1921. https://doi.org/10.1038/srep01921

Chromy, B. A., Nowak, R. J., Lambert, M. P., Viola, K. L., Chang, L., Velasco, P. T. … Klein, W. L. (2003). Self-assembly of Abeta(1–42) into globular neurotoxins. *Biochemistry*, *42*, 12749–12760.

Cizas, P., Budvytyte, R., Morkuniene, R., Moldovan, R., Broccio, M., Losche, M., … Borutaite, V. (2010). Size-dependent neurotoxicity of beta-amyloid oligomers. *Archives of Biochemistry and Biophysics*, *496*, 84–92.

Coitinho, A. S., Freitas, A. R. O., Lopes, M. H., Hajj, G. N. M., Roesler, R., Walz, R., … Brentani, R. R. (2006). The interaction between prion protein and laminin modulates memory consolidation. *European Journal of Neuroscience*, *24*, 3255–3264. https://doi.org/10.1111/j.1460-9568.2006.05156.x

Colognato, H., & Yurchenco, P. D. (2000). Form and function: The laminin family of heterotrimers. *Developmental Dynamics*, *218*, 213–234. https://doi.org/10.1002/(SICI)1097-0177(200006)218:2<213:AID-DVDY1>3.0.CO;2-R

Denman, R., Potempska, A., Wolfe, G., Ramakrishna, N., & Miller, D. L. (1991). Distribution and activity of alternatively spliced Alzheimer amyloid peptide precursor and scrapie PrP mRNAs on rat brain polysomes. *Archives of Biochemistry and Biophysics*, *288*, 29–38. https://doi.org/10.1016/0003-9861(91)90161-B

Diekelmann, S., & Born, J. (2010). The memory function of sleep. *Nature Reviews Neuroscience*, *11*, 114–126. https://doi.org/10.1038/nrn2762

Diociaiuti, M., Macchia, G., Paradisi, S., Frank, C., Camerini, S., Chistolini, P., … Malchiodi-Albedi, F. (2014). Native metastable prefibrillar oligomers are the most neurotoxic species among amyloid aggregates. *Biochimica Et Biophysica Acta*, *1842*, 1622–1629. https://doi.org/10.1016/j.bbadis.2014.06.006

Dohler, F., Sepulveda-Falla, D., Krasemann, S., Altmeppen, H., Schluter, H., Hildebrand, D., … Glatzel, M. (2014). High molecular mass assemblies of amyloid-beta oligomers bind prion protein in patients with Alzheimer's disease. *Brain*, *137*, 873–886.

Dossena, S., Imeri, L., Mangieri, M., Garofoli, A., Ferrari, L., Senatore, A., … Chiesa, R. (2008). Mutant prion protein expression causes motor and memory deficits and abnormal sleep patterns in a transgenic mouse model. *Neuron*, *60*, 598–609. https://doi.org/10.1016/j.neuron.2008.09.008

Ford, M. J., Burton, L. J., Li, H., Graham, C. H., Frobert, Y., Grassi, J., … Morris, R. J. (2002). A marked disparity between the expression of prion protein and its message by neurones of the CNS. *Neuroscience*, *111*, 533–551. https://doi.org/10.1016/S0306-4522(01)00603-0

Graner, E., Mercadante, A. F., Zanata, S. M., Martins, V. R., Jay, D. G., & Brentani, R. R. (2000). Laminin-induced PC-12 cell differentiation is inhibited following laser inactivation of cellular prion protein. *FEBS Letters*, *482*, 257–260. https://doi.org/10.1016/S0014-5793(00)02070-6

Guariniello, L. D., Vicari, P., Lee, K. S., de Oliveira, A. C., & Tufik, S. (2012). Bone marrow and peripheral white blood cells number is affected by sleep deprivation in a murine experimental model. *Journal of Cellular Physiology*, *227*, 361–366. https://doi.org/10.1002/jcp.22743

Guo, T., Noble, W., & Hanger, D. P. (2017). Roles of tau protein in health and disease. *Acta Neuropathologica*, *133*, 665–704. https://doi.org/10.1007/s00401-017-1707-9

Havekes, R., & Abel, T. (2017). The tired hippocampus: The molecular impact of sleep deprivation on hippocampal function. *Current Opinion in Neurobiology*, *44*, 13–19. https://doi.org/10.1016/j.conb.2017.02.005

Ho, J., Tumkaya, T., Aryal, S., Choi, H., & Claridge-Chang, A. (2019). Moving beyond P values: Data analysis with estimation graphics. *Nature Methods*, *16*, 565–566. https://doi.org/10.1038/s41592-019-0470-3

Iqbal, K., del C. Alonso, A., Chen, S., Chohan, M. O., El-Akkad, E., Gong, C.-X., … Grundke-Iqbal, I. (2005). Tau pathology in Alzheimer disease and other tauopathies. *Biochimica Et Biophysica Acta*, *1739*, 198–210. https://doi.org/10.1016/j.bbadis.2004.09.008

Kang, J. E., Lim, M. M., Bateman, R. J., Lee, J. J., Smyth, L. P., Cirrito, J. R., … Holtzman, D. M. (2009). Amyloid-beta dynamics are regulated by orexin and the sleep-wake cycle. *Science*, *326*, 1005–1007.

Koban, M., & Swinson, K. L. (2005). Chronic REM-sleep deprivation of rats elevates metabolic rate and increases UCP1 gene expression in brown adipose tissue. *American Journal of Physiology. Endocrinology and Metabolism*, *289*, E68–74. https://doi.org/10.1152/ajpendo.00543.2004

Lauren, J., Gimbel, D. A., Nygaard, H. B., Gilbert, J. W., & Strittmatter, S. M. (2009). Cellular prion protein mediates impairment of synaptic plasticity by amyloid-beta oligomers. *Nature*, *457*, 1128–1132.

Leng, Y., Musiek, E. S., Hu, K., Cappuccio, F. P., & Yaffe, K. (2019). Association between circadian rhythms and neurodegenerative diseases. *The Lancet Neurology*, *18*, 307–318. https://doi.org/10.1016/S1474-4422(18)30461-7

Liguori, C. (2017). Orexin and Alzheimer's Disease. *Current Topics in Behavioral Neurosciences*, *33*, 305–322.

Liguori, C., Romigi, A., Nuccetelli, M., Zannino, S., Sancesario, G., Martorana, A., … Placidi, F. (2014). Orexinergic system dysregulation, sleep impairment, and cognitive decline in Alzheimer disease. *JAMA Neurol*, *71*, 1498–1505. https://doi.org/10.1001/jamaneurol.2014.2510

Lima, F. R., Arantes, C. P., Muras, A. G., Nomizo, R., Brentani, R. R., & Martins, V. R. (2007). Cellular prion protein expression in astrocytes modulates neuronal survival and differentiation. *Journal of Neurochemistry*, *103*, 2164–2176. https://doi.org/10.1111/j.1471-4159.2007.04904.x

Linden, R., Martins, V. R., Prado, M. A., Cammarota, M., Izquierdo, I., & Brentani, R. R. (2008). Physiology of the prion protein. *Physiological Reviews*, *88*, 673–728. https://doi.org/10.1152/physrev.00007.2007

Loy, A., Follett, L., & Hofmann, H. (2016). Variations of Q-Q Plots: The power of our eyes!. *American Statistician*, *70*, 202–214.

Marshall, L., & Born, J. (2007). The contribution of sleep to hippocampus-dependent memory consolidation. *Trends in Cognitive Sciences*, *11*, 442–450. https://doi.org/10.1016/j.tics.2007.09.001

Mônico-Neto, M., Giampá, S. Q. D. C., Lee, K. S., de Melo, C. M., Souza, H. D. S., Dáttilo, M., … Antunes, H. K. M. (2015). Negative energy balance induced by paradoxical sleep deprivation causes multicompartmental changes in adipose tissue and skeletal muscle. *International Journal of Endocrinology*, *2015*, 1–6. https://doi.org/10.1155/2015/908159

Musiek, E. S. (2015). Circadian clock disruption in neurodegenerative diseases: Cause and effect? *Frontiers in Pharmacology*, *6*, 29. https://doi.org/10.3389/fphar.2015.00029

Necula, M., Kayed, R., Milton, S., & Glabe, C. G. (2007). Small molecule inhibitors of aggregation indicate that amyloid beta oligomerization and fibrillization pathways are independent and distinct. *Journal of Biological Chemistry*, *282*, 10311–10324.

Sandberg, A., Luheshi, L. M., Sollvander, S., de Barros, T. P., Macao, B., Knowles, T. P. J., … Härd, T. (2010). Stabilization of neurotoxic Alzheimer amyloid-beta oligomers by protein engineering. *Proceedings of the National Academy of Sciences of the United States of America*, *107*, 15595–15600.

Sawangjit, A., Oyanedel, C. N., Niethard, N., Salazar, C., Born, J., & Inostroza, M. (2018). The hippocampus is crucial for forming non-hippocampal long-term memory during sleep. *Nature*, *564*, 109–113. https://doi.org/10.1038/s41586-018-0716-8

Spillantini, M. G., & Goedert, M. (2000). The alpha-synucleinopathies: Parkinson's disease, dementia with Lewy bodies, and multiple system atrophy. *Annals of the New York Academy of Sciences*, *920*, 16–27.

Um, J. W., Kaufman, A. C., Kostylev, M., Heiss, J. K., Stagi, M., Takahashi, H., … Strittmatter, S. M. (2013). Metabotropic glutamate receptor 5 is a coreceptor for Alzheimer abeta oligomer bound to cellular prion protein. *Neuron*, *79*, 887–902.

Um, J. W., Nygaard, H. B., Heiss, J. K., Kostylev, M. A., Stagi, M., Vortmeyer, A., … Strittmatter, S. M. (2012). Alzheimer amyloid-beta oligomer bound to postsynaptic prion protein activates Fyn to impair neurons. *Nature Neuroscience*, *15*, 1227–1235.

Wu, H., Dunnett, S., Ho, Y. S., & Chang, R. C. (2019). The role of sleep deprivation and circadian rhythm disruption as risk factors of Alzheimer's disease. *Frontiers in Neuroendocrinology*, *54*, 100764. https://doi.org/10.1016/j.yfrne.2019.100764

Wulf, M. A., Senatore, A., & Aguzzi, A. (2017). The biological function of the cellular prion protein: An update. *BMC Biology*, *15*, 34. https://doi.org/10.1186/s12915-017-0375-5

Yi, C. W., Xu, W. C., Chen, J., & Liang, Y. (2013). Recent progress in prion and prion-like protein aggregation. *Acta Biochimica Et Biophysica Sinica (Shanghai)*, *45*, 520–526. https://doi.org/10.1093/abbs/gmt052

SUPPORTING INFORMATION

Additional supporting information may be found online in the Supporting Information section.

How to cite this article: da Luz MHM, Pino JMV, Santos TG, et al. Sleep deprivation regulates availability of PrP^C and Aβ peptides which can impair interaction between PrP^C and laminin and neuronal plasticity. *J. Neurochem.* 2020;153:377–389. https://doi.org/10.1111/jnc.14960